Preparation and Characterization of Activated Carbon from Hydrochar by Phosphoric Acid Activation and its Adsorption Performance in Prehydrolysis Liquor

Jiachuan Chen,[a,*] Lei Zhang,[a] Guihua Yang,[a,*] Qiang Wang,[a] Rui Li,[a] and
Lucian A. Lucia [a,b]

Hydrochar was used to produce activated carbon with high BET surface area and large pore volume *via* phosphoric acid activation. The hydrochar described here can be obtained from hydrothermal carbonization of corn cob residue (CCR). Porous structure of activated carbons was characterized by nitrogen adsorption and scanning electron microscopy (SEM). Results showed that the specific surface area and total pore volume of activated carbon were increased to 2192 m^2/g and 1.269 cm^3/g, respectively, under conditions of 400 °C, 1 h, and an impregnation ratio of 3, from 5.69 m^2/g and 0.136 cm^3/g of the starting material. The chemical properties of hydrochar and activated carbons were further characterized by Fourier transform infrared spectroscopy (FT-IR), which confirmed the chemical transformation. Furthermore, the localized graphitic nature of the porous carbon was shown by the X-ray diffraction pattern. Thus, the adsorption capacity was enhanced for activated carbon in comparison with commercial carbon. The process of activated carbon preparation provided a high value-added application of hydrochar.

Keywords: Hydrochar; Activated carbons; Specific surface area; Pore volume

*Contact information: a: Key Laboratory of Pulp & Paper Science & Technology of Ministry of Education, Qilu University of Technology, Jinan, Shandong, PR China, 250353; b: The Laboratory of Soft Materials & Green Chemistry, Departments of Forest Biomaterials, Chemistry, North Carolina State University, Raleigh, NC 27695, USA; * Corresponding author: ygh2626@126.com;chenjc@qlu.edu.cn*

INTRODUCTION

Bio-fuel production from biomass waste is generating widespread interest due to the rapid consumption of fossil-based fuels and growing concerns of environmental pollution (Yang *et al.* 2013a, 2013b; Wang *et al.* 2014). Two major thermochemical treatments, hydrothermal carbonization (HTC) and high-temperature pyrolysis, can achieve the conversion from biomass to bio-fuel (Karagoz *et al.* 2005; Zhang *et al.* 2013). Compared to a pyrolysis treatment, hydrothermal carbonization has great potential for converting lignocelluloses into bio-fuel and novel carbon materials due to several advantages, such as the production of liquefied components, high conversion efficiency, and relatively low operation temperature; also, there is no need to use toxic chemicals. HTC was first introduced by Bergius in 1913 who described the hydrothermal transformation of cellulose into coal-like materials (Bergius 1913). Typically, the process consists of the heat treatment of an aqueous solution/dispersion of organic materials under autogenous pressure at temperatures as low as 150 to 350 °C. The resulting solid carbon products (hydrochars) generally exhibit uniform chemical and structural properties as well as very high and tunable content of oxygen-containing functional groups; and the yield of hydrochars is about 70 to 80%, which is higher than pyrolysis. Consequently, a variety of these functional carbonaceous materials have been synthesized from biomass *via* the HTC process for potential applications in energy storage (Cakan *et al*. 2008), water purification (Hu 2010), hydrogen storage (Titirici *et al*. 2012), and catalysis (Titirici and Antonietti 2010).

Actually, HTCs are somewhat not "real" carbon materials as a result of their low carbon content (<80%) (Krishnan *et al*. 2013). The HTCs directly derived from carbohydrates usually suffer from a low specific surface area (SSA) (S_{BET}<10 m^2 g^{-1}) and poor electro-conductivity, resulting in restricted applications in purification and energy storage (Wei *et al*. 2011). In this regard, an activation method is usually introduced to improve the porosity and SSA of HTCs. Activated carbons have been used extensively in various fields, such as industrial purification, chemical recovery operations, catalyst supports, and electrode materials for batteries and electrochemical capacitors, due to their large specific surface area, highly porous structure, and ability to be easily regenerated for reuse. Activated carbons are mainly obtained through the chemical and physical activation of hydrochar. Physical activation is performed in two steps: carbonization of the precursor and activation of resulting char with carbon dioxide, steam *etc*. Chemical activation also involves two stages: impregnation of a precursor with chemical activating agents, such as phosphoric acid, zinc chloride, potassium hydroxide, *etc*., and activation of the mixture at temperatures 300 °C to 800 °C under a N_2 atmosphere. To obtain a high surface area and large pore volume in activated carbons, chemical activation demonstrates a better performance than physical activation. Alkali hydroxides are usually used to prepare high surface area and large volume porous carbons. Zheng *et al.* (2014) reported that the highly porous carbon nanosheets having a large surface area (2633 m^2 g^{-1}) and a high pore volume (1.86 cm^3 g^{-1}) are prepared by a one-step KOH activation of glucose hydrochar spheres. However, the strong alkalinity of KOH, as well as some hazardous by-products, is harmful for the environment, and the activation agents could not be recovered easily in industry. Consequently, phosphoric acid is the preferred activation agent due to its mild reaction conditions and recyclable properties (Guastalli *et al.* 2009). Nahil and Williams (2012) produced activated carbon with a BET surface area of 1720 m^2/g using phosphoric acid activation of cotton stalk. Myglovetsa *et al.* (2014) reported that the maximum value, 1370 m^2/g, of BET surface area of can be achieved at a temperature of 1000 °C when producing a carbon adsorbent from lignosulfonate by phosphoric acid activation.

The pre-hydrolysis process has been widely used prior to kraft pulping for producing dissolving pulp. In this process, biomass is treated with hot water or steam that removes most hemicelluloses from wood chips. The pre-hydrolysis liquor (PHL) that is produced in this process is currently mixed with black liquor (*i.e.* spent liquor) and combusted in the recovery process or treated in the wastewater of the process (Liu *et al*. 2011). In the current practice, the extracted hemicellulose of PHL is under-utilized. Interestingly, the hemicelluloses can be converted to biofuel *via* bioconversion pathways (Fatehi *et al*. 2013). However, lignin, furfural, and acetic acid have been reported to be inhibitors for conversion of sugars to biofuels. Different methods were proposed in the literature to remove the inhibitors of PHL for improving the efficiency of biofuel production from PHL (Liu *et al*. 2012). Adsorption can also be employed as a means to remove inhibitors from PHL. The application of activated carbon as an adsorbent in extracting lignocelluloses from industrial wastes was stated previously (Liu *et al*. 2014).

In this study, the hydrochar obtained from hydrothermal carbonization of corncob residual (CCR) was chosen as a new carbon precursor for high-performance activated carbon through phosphoric acid activation. The main objective was to investigate the influence of different impregnation ratios, activation temperatures, and activation times on the production of activated carbons. The hydrochar derived porous carbons were systematically characterized by Fourier transform infrared spectroscopy (FT-IR), scanning electron microscopy (SEM), and surface area analysis. Its adsorption performance in prehydrolysis liquor (PHL) of kraft-based dissolving pulp production was further studied.

EXPERIMENTAL

Materials

Industrially produced CCR was collected from a furfural production mill located in Shandong, China. The CCR was milled into 100-mesh particle sizes after air-drying. The chemical composition, such as cellulose 72.3%, lignin 16.2%, hemicellulose 7.2%, extractives 8.1%, and ash 4.2%, was reported in an earlier report (Zhang *et al.* 2015b). The PHL was obtained from a plant in Shandong, China that produces kraft-based dissolving pulp using poplar. Commercially activated carbon powder, sulfuric acid, phosphoric acid, and hydrochloric acid (analytical grade) was purchased from Fu Yu Fine Chemical Co. Ltd. (Tianjin, China).

Preparation of Hydrochar

The hydrochar used in this study was obtained according to the authors' previous study (Zhang *et al.* 2015). Briefly, CCR (equivalent to oven-dried weight) and deionized water were added into a 250-mL Parr stirred pressure reactor, and nitrogen gas was used to purge the air inside the reactor. The reactor was heated to 250 °C and maintained for 4 h at a stirring rate of 150 rpm, followed by cooling to room temperature. The hydrochar was recovered by filtration and washed with ethanol and deionized water until the filtrate was colorless, then oven-dried at 105 °C for 24 h.

Preparation of activated carbon

The hydrochar was impregnated with 85% phosphoric acid. The impregnated ratios of H_3PO_4/hydrochars were 1.5, 2, 3, 4, and 6. After sufficient mixing, the acid-impregnated sample was dried overnight at 90 °C. Then the sample was transferred to a tube furnace and heated to the activation temperature (300 °C to 700 °C) at a rate of 5 $°C \cdot min^{-1}$ and maintained at a corresponding temperature for 0.5 h to 4 h under N_2 atmosphere. After activation, the porous carbon was cooled down to room temperature under nitrogen flowing. The resulting product was placed in 200 mL of 1 M HCl solution and boiled for 1 h. Finally, the product was washed to a neutral pH and oven-dried overnight at 105 °C to obtain the activated carbon.

Methods

Characterization of activated carbon

Nitrogen gas sorption isotherms of hydrochar and activated carbons were collected at -196 °C using v-sorb 2800p sorptometer (Beijing, China). The isotherm date was recorded at relative pressures (P/P_0) in the range of 10^{-6} to 0.99. The surface area

(S_{BET}) was calculated by the standard BET method based on adsorption data in the relative pressure (P/P_0) range 0.06 to 0.18 and the total pore volume was calculated from the amount of nitrogen adsorbed at a relative pressure (P/P_0) of 0.99. The micropore volume was determined by the t-plot method and the mesopore volume was calculated by deducting the micropore volume from the total pore volume. The Density Functional Theory (DFT) method was applied to obtain the pore size distributions using nitrogen adsorption data.

The reflectance infrared spectra were obtained on a Shimadzu FT-IR spectrophotometer (Kyoto, Japan). Each spectrum was recorded over a wavenumber range of 500 cm^{-1} to 4000 cm^{-1}. Oven-dried KBr pellets were used for sample preparation.

The surface morphology was examined by SEM (QUNTA 200, FEI Corporation, Hillsboro, OR, USA). All of the samples were prepared by a sputter coater (SCD 005, Switzerland BAL-TEC Corporation, Pfäffikon, Switzerland) under an accelerating voltage of 15 kW.

Adsorption studies

Approximately 100 mL of PHL was added to 1 g of produced and commercial ACs in a 250 mL Erlenmeyer flask, and shaken for 24 h at 150 rpm under 25 °C. Then, the samples were filtered by the cellulose nitrate membrane (0.45 μm) for further analysis.

PHL analysis

The sugars were determined using an ion chromatography unit (IC) (ICS-5000, Thermo Fisher Corporation, Waltham, MA, USA) equipped with a CarboPac PA20 column and an autosampler. To convert the oligosaccharides of PHL to monosaccharides, additional acid hydrolysis of the sample was performed under the conditions of 4% sulfuric acid at 121 °C in an oil bath for 1 h. The detector used integrated pulsed amperometric detection, and the waveform was a standard quad for carbohydrates. Approximately 2 mmol/L NaOH was used as the regeneration agent at 0.5 mL/min, and 200 mmol/L NaOH to flush the column. The samples were filtered and diluted prior to analysis.

The lignin was measured based on the UV/Vis spectrometric method at a wavelength of 205 nm. The concentrations of furfural in the original PHL and filtrates were determined by a high performance liquid chromatography (HPLC) (Shimadzu LC-20AT, Kyoto, Japan) unit equipped with a SHIM-PACK VP ODS column (250*4.6 mm, Shimadzu, Kyoto, Japan) and a UV detector (SPD-20A). The column temperature and the detector temperature were both set to 35 °C. The wavelength used was 270 nm. Approximately 0.1% H_3PO_4 was used as the mobile phase A, and 50% methanol and 50% methyl cyanide as the mobile phase B at a 1.0 mL/min flow rate.

RESULTS AND DISCUSSION

Proposed Process for Hydrothermal Treatment of Corn Cob and Inhibitors Removal from PHL by Activated Carbon Based Hydrochar

During the pre-hydrolysis step, the majority of hemicelluloses are removed and dissolved in the liquor, along with other organic compounds, such as acetic acid, lignin, and furfural. Effectively recovering these components will make it viable for the biorefinery concept of dissolving pulp production process. However worse still, lignin and furfural in PHL inhibit the fermentation of hemicellulose to value-added products, *e.g*. ethanol and xylitol (Helmerius *et al*. 2010). To facilitate the application of the lignocellulose of PHL in the production of value-added products, the amounts of inhibitors in the PHL need to be minimized.

Corn is vastly used as food or for biochemical products. In these processes, corn cob is considered as waste, but it can be converted to value-added products, such as xylitol, xylooligosaccharides, and furfural. Meanwhile, corncob residual (CCR), as a hemicellulose-depleted waste residue, is produced during the corn cob conversion process, as shown in Fig 1. The lignin and cellulose remaining in CCR makes it a promising lignocellulosic material for bio-fuel, platform chemicals, and functional carbonaceous materials. As a value-added chemical, activated carbon has extensive industrial applications. Alternatively, adsorption by activated carbon can be considered for removing the inhibitors from PHL. Figure 1 illustrates a proposed process diagram of hydrothermal treatment of corn cob and inhibitors removal from PHL by activated carbon based corn cob residual hydrochar integrated with the furfural, xylitol, and xylooligosaccharide production process. HTC is now being mentioned as a promising technology to convert corn cob residual into multiple bioproducts: gases, such as CO_2, nitrogen oxides, and sulfur oxides, dissolve into water, forming corresponding acids and salts, eliminating air pollution treatment schemes; liquid fuel or bio-oil, containing sugar-derived compounds, and lignin-derived compounds, may be potentially used for biochemicals and biomaterials; the hydrochar is a kind of carbon material that could be activated to work as an adsorbent for PHL purification.

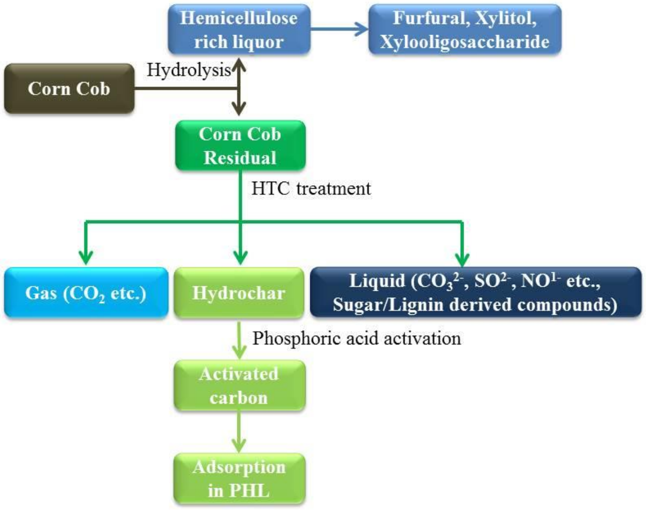

Fig. 1. Proposed integration for inhibitors adsorbed by activated carbon based the process of hydrothermal carbonization of CCR in a kraft-based dissolving pulp production process

Yield of Activated Carbon

The yield of the activated carbon is defined as the ratio of the weight of activated carbon after activation, washing and drying to the weight of the dried corn cob residue. As can be seen from Table 1, as the activation temperature increased from 300 to 700 °C, the activated carbon yield decreased from 37.4 to 29.4. This was due to the loss of volatile materials with increasing pyrolysis temperature. The presence of phosphoric acid during activation promotes the depolymerization, dehydration, and redistribution of constituent biopolymers, thus increasing the yield of activated carbon (Prahas *et al*. 2008). At the carbonization temperature of 400 °C, activation with a H_3PO_4 impregnation ratio of 3 resulted in a highest yield of 35.5. The activated carbon yields decreased with increasing impregnation ratio. The phosphoric acid reacted with the char and volatile matter and diffused quickly out of the surfaces of particles during the activation process (Yorgun and Yıldız 2015). Therefore, with a high phosphoric acid content, the gasification of surface carbon atoms became predominant, leading to an increase in the weight loss and a low carbon yield. Besides, at the activation temperature of 400 °C and impregnation ratio of 3, the activation time has a slight effect on activated carbon with a range of 32.5-35.5.

Effect of Impregnated Ratios on Surface Area and Pore Volume

The effect of impregnated ratios on the textural parameters of the activated carbons at 400 °C for 1 h were investigated and listed in Table 1. Phosphoric acid as an activating agent was found to be very efficient in the production of activated carbons with high porosity and the impregnation ratio has a significant influence on porosity development. It can be seen that the BET surface area and total pore volumes of activated carbons increased from 1580 m^2/g and 0.786 cm^3/g to 2192 m^2/g and 1.269 cm^3/g as the impregnation ratio increased from 1.5 to 3. Then, they decreased to 1237 m^2/g and 0.693 cm^3/g at a ratio of 6. This might have been caused by the change in the contact area between the hydrochar and phosphoric acid, which was affected by the impregnation ratio. The higher impregnation ratio would lead to the expansion of the pore structure, which initiated the collapse of the pores and structural contraction (Castro *et al*. 2000; Sych *et al.* 2012). Additionally, higher phosphate acid concentrations will form a protective layer to prevent the activating agent incorporating into the hydrochar, thus hindering any increases in specific surface area and total pore volume (Nahil and Williams 2012). A similar phenomenon was also observed by Nahil and Williams (2012) when using phosphoric acid activation of cotton stalks; AC was produced with a BET surface area of 1720 m^2/g and a total pore volume of 0.89 cm^3/g at an impregnation ratio of 1.5 and 500 °C.

Effect of Activation Temperature on Surface Area and Pore Volume

The BET surface areas, micropore volume, mesopore volume, and total pore volume of activated carbons prepared at different activation temperatures are listed in Table 1. As shown, the BET surface area and total pore volumes increased when the temperature increased from 300 °C to 400 °C, followed by a decrease in BET surface area and total pore volumes from 400 °C to 700 °C. The BET surface area and total pore volumes reached the maximum values of 2192 m^2/g and 1.269 cm^3/g at the activation temperature of 400 °C. According to the Jagtoyen and Derbyshire (1998) study on the H_3PO_4 activation of hardwoods, the phosphate ester cross-linked structure forms and expands as the temperature rises in the lower temperature range of 200 °C to 450 °C, and then began to break down, causing contraction and a decrease in the surface area and pore volumes at higher temperatures above 450 °C. Similarly, Castro *et al*. (2000) observed that the surface area and pore volumes were highly dependent on the temperature when using agricultural residues for activated carbon production.

Effect of Activation Time on Surface Area and Pore Volume

The effect of activation time on activated carbons prepared is shown in Table 1. The results indicated that BET surface area and total pore volumes of activated carbon reached a maximum value of 2192 m^2/g and 1.269 cm^3/g for the activation time of 1 h. Then, the BET surface area and total pore volume decreased to 1615 m^2/g and 0.95 cm^3/g when the activation time was prolonged to 4 h. This could have been explained by the excessive time that led to the contraction and collapse of pores, thus the surface area and pore volume became smaller (Wang *et al.* 2011). The effect of activation time on activated carbons was also reported by Castro *et al.* (2000), that prolongation of activation time beyond 1 h led to a pronounced reduction in porosity development.

Table 1. Textural Parameters of the Activated Carbons

Impregnation Ratio/Temperature (°C)/Time (h)	Yield (%)	Textural Parameters				
		S_{BET} (m^2/g)	V_{mic} (cm^3/g)	V_{mes} (cm^3/g)	V_{total} (cm^3/g)	V_{mic} (%)
Hydrochar	42.2	5.69	0	0.136	0.136	0
1.5/400/1	29.5	1580	0.667	0.119	0.786	85%
2/400/1	30.1	1619	0.703	0.222	0.925	76%
3/400/1	35.5	2192	0.856	0.413	1.269	67%
4/400/1	31.0	1896	0.687	0.338	1.025	67%
6/400/1	30.6	1237	0.472	0.221	0.693	68%
3/300/1	37.4	1601	0.640	0.396	1.036	62%
3/500/1	34.0	1768	0.725	0.387	1.112	65%
3/600/1	33.1	1474	0.661	0.230	0.891	74%
3/700/1	29.4	1459	0.664	0.233	0.897	74%
3/400/0.5	33.1	1955	0.832	0.277	1.109	75%
3/400/1.5	34.0	1812	0.704	0.207	0.911	77%
3/400/2	33.0	1663	0.698	0.265	0.963	72%
3/400/4	32.5	1615	0.711	0.239	0.950	75%

N_2 Adsorption-desorption Isotherms of Activated Carbons

The nitrogen adsorption-desorption isotherms of the activated carbons obtained are shown in Fig. 2a, b, and c. The isotherms of the porous carbons were classified into type I, which associated with the microporous structure according to the IUPAC (International Union of Pure and Applied Chemistry) classification. The volume of adsorbed N_2 increased rapidly at relative pressures lower than 0.1, which indicated that porous carbons had a large number of microporous structures. Furthermore, the amount of adsorbed N_2 did not increase greatly at relative pressures higher than 0.1, which suggested that the mesoporous structures were less developed. The difference of the volumes of adsorbed N_2 indicated that the adsorption capacity varied with different impregnation ratios (Fig. 2a). With the impregnation ratio increased from 1.5 to 3, the adsorption capacity of N_2 improved gradually, which indicated a correlation between the impregnation ratio, BET surface area, and total pore volume. Figure 2b illustrates that the adsorption capacity of activated carbon was enhanced when the activation temperature increased from 300 °C to 400 °C. However, the amount of N_2 adsorbed decreased for the activated carbons with temperatures increased beyond 400 °C. This phenomenon confirmed that the higher temperature led to the contraction and the collapse of pores. Figure 2c shows the adsorption-desorption isotherms of the activated carbons prepared at

0.5 h to 4 h under an activation temperature of 400 °C and impregnation ratio of 3. The adsorption capacity of N_2 reached its maximum at activation time of 1 h. However, little N_2 adsorption improvement was found when activation time was further prolonged beyond 1.5 h.

Fig. 2b, 2d, and 2f show DFT pore size distributions for activated carbons prepared at different impregnation ratios, different activation temperature, and time, respectively. The pore size distribution (PSD) plot reflected a hierarchical porous architecture with a maximum at around 2.2 nm for all samples. This indicates that the chemical activation of hydrochars resulted in development of micropores. The intensity of these peaks at around 2.2 nm is directly related to the impregnation ratio, activation temperature and time. It can be seen that the activated carbon produced at an impregnation ratio of 3, activation temperature of 400 °C and time of 1 h shows the strongest peak at pore width 2.2 nm compared with activated carbons obtained under other conditions.

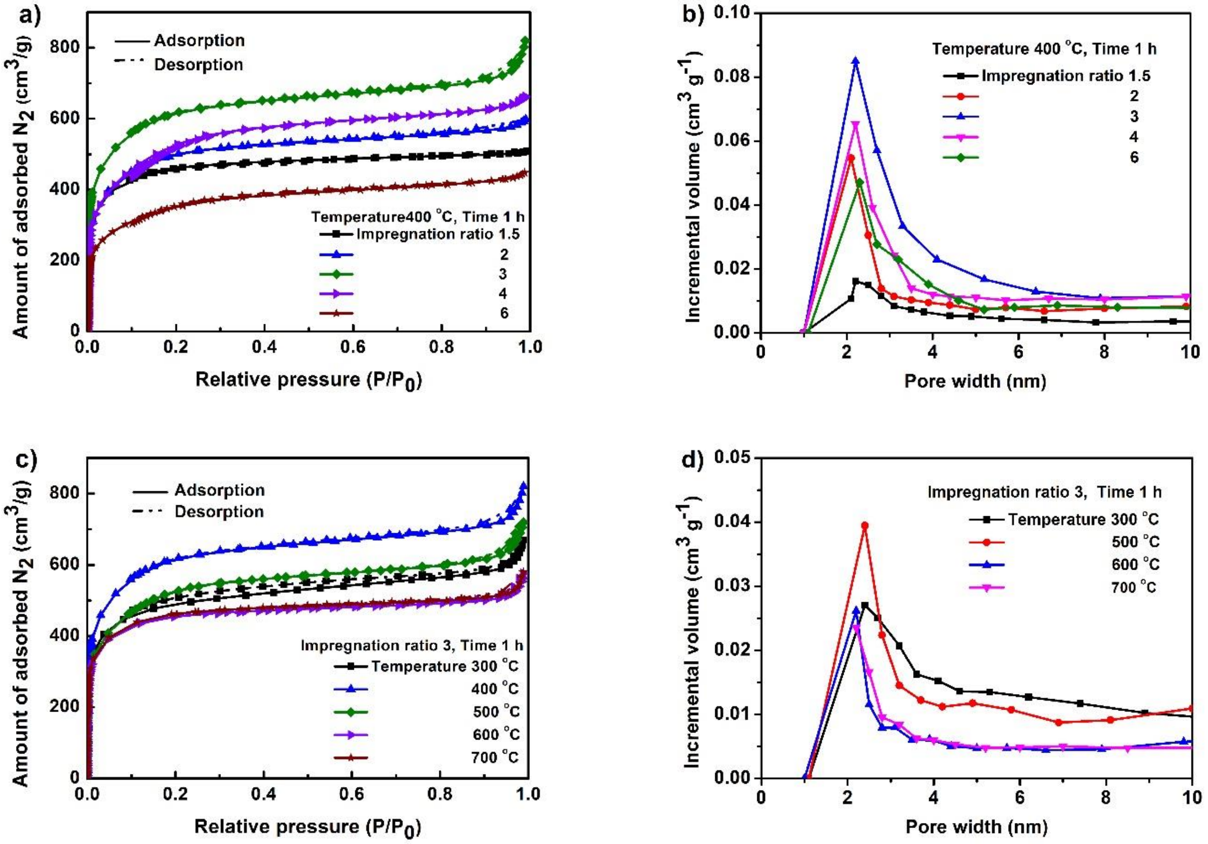

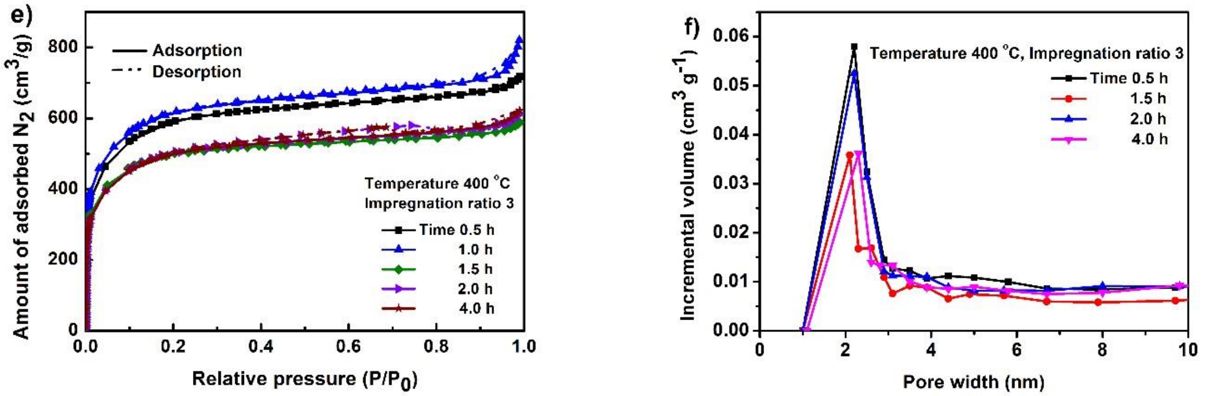

Fig. 2. N_2 adsorption-desorption isotherms and DFT pore size distribution of activated carbons with different impregnation ratios prepared at 400 °C, 1 h (a, b) and carbons prepared with impregnation ratio of 3 at different activation temperatures (c, d) and at different activation time (e, f)

Surface Morphology Studies

The SEM images of CCR (a), hydrochar (b), and AC (c), at 400 °C for 1 h under an impregnation ratio of 3 are shown in Fig. 3. As shown, the surface of CCR was relatively smooth while having small pores, which may have been caused by the recombination of carbon products from decarboxylation reactions and release of volatiles during the carbonization process (Liu *et al.* 2011; Zhang *et al*. 2015a). Figure 2b shows that a large number of microspheres were aggregated on the surface. This might have been caused by the polymerization during hydrothermal carbonization. In contrast, the irregular structure of cavities and pores were clear for the H_3PO_4 activated AC (Fig. 2c). Also, a large number of small carbon pieces were accumulated together on the AC surface, which might have been caused by the combination of biopolymers fragments during carbonization process (Solum *et al.* 1995; Castro *et al.* 2000). Patnukao and Pavasant (2008) also observed the irregular structure of cracks and crevices on the AC surface when using phosphoric acid activation of *Eucalyptus camaldulensis* Dehnh. bark.

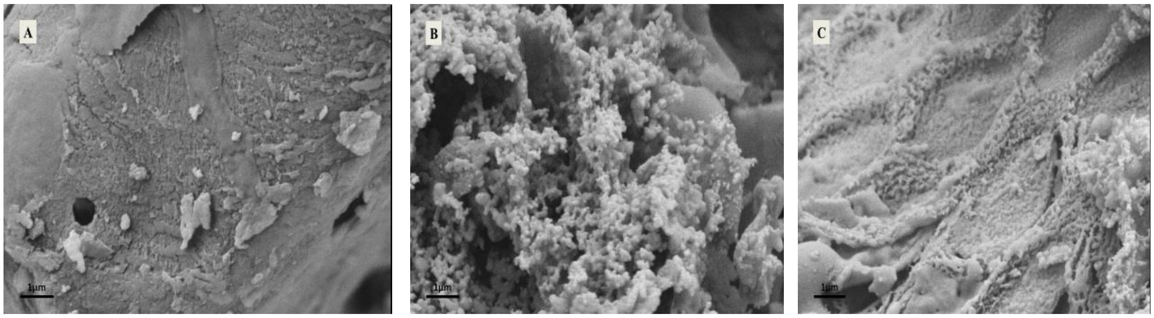

Fig. 3. SEM images of the CCR (A), hydrochar (B), and AC (C) produced at an impregnation ratio of 3, 400 °C, and after 1 h

FT-IR Spectra

The FT-IR spectra of hydrochar and ACs obtained at the different impregnation ratios are shown in Fig. 4. As shown, all the ACs have similar infrared spectra, which indicated the parallel chemical nature of the functional groups. The bands located in the range of 3000 cm^{-1} to 4000 cm^{-1} attributed to the functional groups of O-H stretching vibrations of phenol, alcohol, and carboxylic acid (Martins *et al.* 2007; El-Hendawy *et al.* 2008). The band at about 2900 cm^{-1} belonged to C-H stretching in methyl and methylene groups (Özhan *et al.* 2014). The C=O stretching in lactones and C=C stretching in olefins could be found at about 1700 cm^{-1} and 1610 cm^{-1}, respectively (Shafeeyan *et al.* 2010).

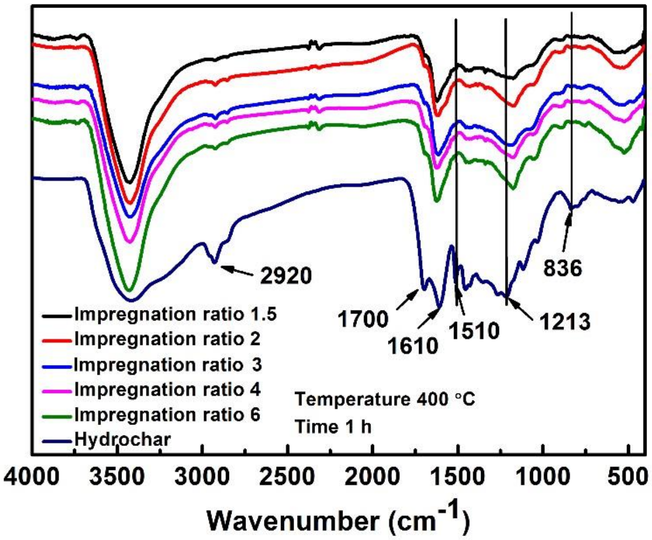

Fig. 4. FTIR spectra for the hydrochar and ACs produced under different impregnation ratios, 400 °C, and 1 h

The absorbance peak at about 1510 cm^{-1} may have been due to C-O stretching in carbonyls, carboxylic acid, and lactones. Moreover, the absorbance bands of hydrochar between 750 cm^{-1} to 1000 cm^{-1} and 1100 cm^{-1} to 1600 cm^{-1} were different with ACs that confirmed the chemical transformation occurred during the phosphoric acid activation process. The noticeable chemical difference between the starting material and produced AC was also observed by Myglovetsa *et al.* (2014).

XRD Analysis

The crystalline structures of the hydrochar and the different activated carbons (activation temperature and time were 400 °C and 1 h, different impregnation ratios) were investigated by XRD (Fig. 5). The X-ray diffraction patterns show broad asymmetric diffraction peaks that are located at approximately 2θ=25°, indicating the formation of turbostratic structure of disordered carbon. A weak peak at 2θ=43° also emerged in the patterns of activated carbons; this can be indexed to diffraction from the (100) planes of graphite (JCPDS Card No. 41-1487), indicating that the activated carbons prepared under the temperature of 400 °C have a low degree of graphitization. It was impossible to completely graphitize in such low-temperature, so the macroscopy of the activated carbons show an amorphous structure.

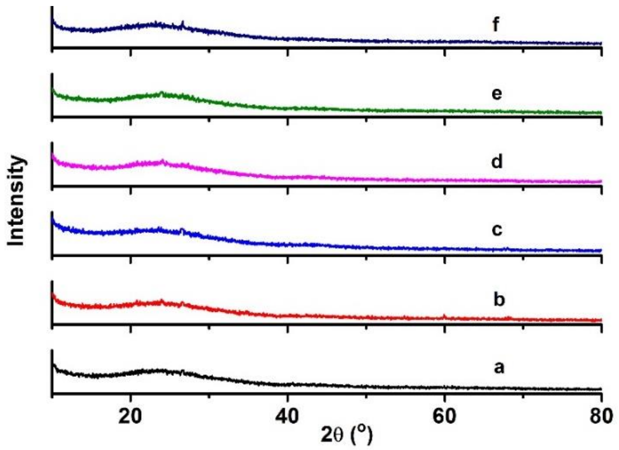

Fig. 5. XRD patterns of hydrochar and the activated carbons prepared at different impregnation ratio: (a)-1.5, (b)-2, (c)-3, (d)-4, (e)-6 and (f)-hydrochar

Adsorption on ACs

Figure 6 shows the adsorption performance on saccharides, lignin, and furfural on produced activated carbons in PHL. Evidently, the activated carbon prepared under the condition of impregnation ratios of 3 and 400 °C for 1 h manifested the maximum adsorption capacity that 53.5% of lignin and 41.7% of furfural were removed from the PHL corresponding the maximum adsorption of lignin and furfural were 830 mg/g and 70 mg/g on activated carbon. The pronounced adsorption performance of AC-3/400/1 could be attributed to its high surface area, high microporous surface, and small mesopore diameters. These results imply that the adsorption using activated carbon is very selective in removing inhibitors from PHL. In addition, 21.9% of the saccharides were also removed from the PHL. Previous studies have found that the lignin-carbohydrate complexes (LCCs) could be formed during hydrolysis, suggesting that LCCs were present in the PHL (Liu *et al*. 2012; Tunc *et al*. (2010)). Therefore, a part of saccharides removal might be due to adsorption of LCCs onto activated carbons.

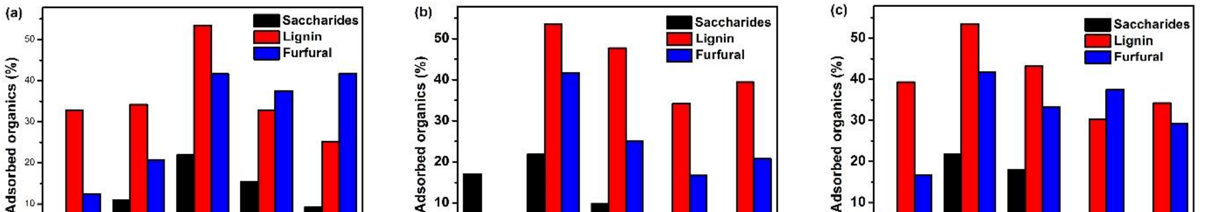

Fig. 6. Adsorption performance of activated carbons in PHL

CONCLUSIONS

1. The activated carbon production from hydrochar of hydrothermally-treated CCR based on phosphoric acid activation was investigated. The optimal conditions were an impregnation ratio of 3, temperature of 400 °C, and activation time of 1 h. These

conditions yielded the AC with a BET surface area of 2192 m^2/g and pore volume of 1.269 cm^3/g.

2. The N_2 adsorption isotherms and SEM images of porous carbons confirmed the well-developed micropore structure.
3. The chemical changes of AC during activation process, which were detected by FT-IR and X-ray diffraction patterns, indicated that the activated carbons prepared under the temperature of 400 °C have a low degree of graphitization.
4. A higher adsorption capacity for impurity removal in PHL was achieved for produced AC in comparison with the commercial one.

ACKNOWLEDGMENTS

The authors are grateful for the financial support from the National Science Foundation of China (Grant Nos. 31470602, 31670595, 31670584), and the Taishan Scholars Program of Shandong Province.

REFERENCES CITED

Bergius, F. (1913). "Formation of anthracite," *Z. Elektrochem.* 19, 858-860.

Castro, J. B., Bonelli, P. R., Cerrella, E. G., and Cukierman, A. L. (2000). "Phosphoric acid activation of agricultural residues and bagasse from sugar cane: Influence of the experimental conditions on adsorption characteristics of activatedcarbons," *Industrial & Engineering Chemistry Research* 39(11), 4166-4172. DOI: 10.1021/ie0002677

Cakan, R. D., Titirici, M. M., Antonietti, M., Cui, G. L., Maier, J., and Hu, Y. S. (2008). "Hydrothermal carbon spheres containing silicon nanoparticles: Synthesis and lithium storage performance," *Chemical Communications* 32, 3759-3761. DOI: 10.1039/B805671B

Fatehi, P., Ryan, J., and Ni, Y. (2013). "Adsorption of lignocelluloses of model pre-hydrolysis liquor on activated carbon," *Bioresource Technology* 131, 308-314. DOI: 10.1016/j.biortech.2012.12.156

Guastalli, A. R., Labanda, J., and Llorens, J. (2009). "Separation of phosphoric acid from an industrial rinsing water by means of nanofiltration," *Desalination* 243, 218-228. DOI: 10.1016/j.desal.2008.04.024

Helmerius, J., von Walter, J. V., Rova, U., Berglund, K. A., and Hodge, D. B. (2010). "Impact of hemicellulose pre-extraction for bioconversion on birch kraft pulp properties," *Bioresource Technology* 101(15), 5996-6005. DOI: 10.1016/j. biortech. 2010.03.029

Hu, B., Wang, K., Wu, L., Yu, S. H., Antonietti, M., and Titirici, M. M. (2010). "Engineering carbon materials from the hydrothermal carbonization process of biomass," *Advanced Materials* 22(7), 813-828. DOI: 10.1002/adma.200902812

Jagtoyen, M., and Derbyshire, F. (1998). "Activated carbons from yellow poplar and white oak by H_3PO_4 activation," *Carbon* 36(7-8), 1085-1097. DOI: 10.1016/S0008-6223(98)00082-7

Karagoz, S., Bhaskar, T., Muto, A., and Sakata, Y. (2005). "Comparative studies of oil compositions produced from sawdust, rice husk, lignin and cellulose by hydrothermal treatment," *Fuel* 84(7-8), 875-884. DOI: 10.1016/j.fuel.2005.01.004

Krishnan, D., Raidongia, K., Shao, J., and Huang, J. (2013). "Graphene oxide assisted hydrothermal carbonization of carbon hydrates," *ACS Nano* 8(1), 449-457. DOI: 10.1021/nn404805p

Liu, H., Hu, H., Jahan, M. S., Baktash, M. M., and Ni, Y. (2014). "Purification of hemicelluloses in pre-hydrolysis liquor of kraft-based dissolving pulp production process using activated carbon and ion-exchange resin adsorption followed by nanofiltration," *Journal of Biobased Materials and Bioenergy* 8(3), 325-330. DOI: 10.1166/jbmb.2014.1438

Liu, X., Fatehi, P., and Ni, Y. (2011). "Adsorption of lignocelluloses dissolved in prehydrolysis liquor of kraft-based dissolving pulp process on oxidized activated carbons," *Industrial & Engineering Chemistry Research* 50(20), 11706-11711. DOI: 10.1021/ie201036q

Liu, X., Fatehi, P., and Ni, Y. (2012). "Removal of inhibitors from pre-hydrolysis liquor of kraft-based dissolving pulp production process using adsorption and flocculation processes," *Bioresource Technology* 116, 492-496. DOI: 10.1016/j.biortech. 2012. 03. 069

Myglovetsa, M., Poddubnayaa, O. I., Sevastyanovac, O., Lindström, M. E., Gawdzikd, B., Sobiesiakd, M., Tsyba, M. M., Sapsaye, V. I., Klymchuke, D. O., and Puziya, A. M. (2014). "Preparation of carbon adsorbents from lignosulfonate by phosphoric acid activation for the adsorption of metal ions," *Carbon* 80, 771-783. DOI: 10.1016/ j.carbon.2014.09.032

Nahil, M. A., and Williams, P. T. (2012). "Pore characteristics of activated carbons from the phosphoric acid chemical activation of cotton stalks," *Biomass and Bioenergy* 37, 142-149. DOI: 10.1016/j.biombioe.2011.12.019

Patnukao, P., and Pavasant, P. (2008). "Activated carbon from eucalyptus camaldulensis dehn bark using phosphoric acid activation," *Bioresource Technology* 99(17), 8540-8543. DOI: 10.1016/j.biortech.2006.10.049

Prahas, D., Kartika, Y., Indraswati, N., and Ismadji, S. (2008). "Activated carbon from jackfruit peel waste by H_3PO_4 chemical activation: pore structure and surface chemistry characterization," *Chemical Engineering Journal* 140(1), 32-42. DOI: 10.1016/j.cej.2007.08.032

Solum, M. S., Pugmire, R. J., Jagtoyen, M., and Derbyshire F. (1995). "Evolution of carbon structure in chemically activated wood," *Carbon* 33(9), 1247-1254. DOI: 10.1016/0008-6223(95)00067-N

Sych, N. V., Trofymenko, S. I., Poddubnaya, O. I., Tsyba, M. M., Sapsay, V. I., Klymchuk, D. O., and Puziy, A. M. (2012). "Porous structure and surface chemistry of phosphoric acid activated carbon from corncob," *Applied Surface Science* 261, 75-82. DOI: 10.1016/j.apsusc.2012.07.084

Titirici, M. M., and Antonietti, M. (2010). "Chemistry and materials options of sustainable carbon materials made by hydrothermal carbonization," *Chemical Society Reviews* 39(1), 103-116. DOI: 10.1039/B819318P

Titirici, M. M., White, R. J., Falco, C., and Sevilla, M. (2012). "Black perspectives for a green future: hydrothermal carbons for environment protection and energy storage," *Energy & Environmental Science* 5(5), 6796-6822. DOI:10.1039/C2EE21166A

Tunc, M. S., Lawoko, M., and van Heiningen, A. R. (2010). "Understanding the limitations of removal of hemicelluloses during autohydrolysis of a mixture of southern hardwoods," *BioResources* 5(1), 356-371.

Wang, L., Guo, Y., Zou, B., Rong, C., Ma, X., Qu, Y., Li, Y., and Wang, Z. (2011). "High surface area porous carbons prepared from hydrochars by phosphoric acid activation," *Bioresource Technology* 102(2), 1947-1950. DOI: 10.1016/ j. biortech. 2010.08.100

Wang, Q., Jahan, M. S., Liu, S., Miao, Q., and Ni, Y. (2014). "Lignin removal enhancement from prehydrolysis liquor of kraft-based dissolving pulp production by laccase-induced polymerization," *Bioresource Technology* 164, 380-385. DOI: 10.1016/j.biortech.2014.05.005

Wei, L., Sevilla, M., Fuertes, A. B., Mokaya, R., and Yushin, G. (2011). "Hydrothermal carbonization of abundant renewable natural organic chemicals for high-performance supercapacitor electrodes," *Advanced Energy Materials* 1(3), 356-361. DOI: 10.1002/aenm.201100019

Yang, G., Jahan, M. S., Ahsan, L., and Ni, Y.(2013a). "Influence of the diluent on the extraction of acetic acid from the prehydrolysis liquor of kraft based dissolving pulp production process by tertiary amine," *Separation and Purification Technology* 120, 341-345. DOI: org/10.1016/j.seppur.2013.10.003

Yang, G., Jahan, M. S., Ahsan, L., Zheng, L., and Ni, Y. (2013b). "Recovery of acetic acid from pre-hydrolysis liquor of hardwood kraft-based dissolving pulp production process by reactive extraction with triisooctylamine," *Bioresource Technology* 138, 253-258. DOI: 10.1016/j.biortech.2013.03.164

Yorgun, S., and Yıldız, D. (2015). "Preparation and characterization of activated carbons from paulownia wood by chemical activation with H_3PO_4," *Journal of the Taiwan Institute of Chemical Engineers* 53, 122-131. DOI: 10.1016/j.jtice.2015.02.032

Zhang, L., Liu, R., Yin, R., and Mei, Y. (2013). "Upgrading of bio-oil from biomass fast pyrolysis in China: A review," *Renewable and Sustainable Energy Reviews* 24, 66-72. DOI: 10.1016/j.rser.2013.03.027

Zhang, L., Liu, S., Wang, B., Wang, Q., Yang, G., and Chen, J. (2015a). "Effect of residence time on hydrothermal carbonization of corn cob residual," *BioResources* 10(3), 3979-3986.

Zhang, L., Wang, Q., Wang, B., Yang, G., Lucia, L. A., and Chen, J. (2015b). "Hydrothermal carbonization of corncob residues for hydrochar production," *Energy & Fuels* 29(2), 872-876. DOI: 10.1021/ef502462p

Zheng, X., Lv, W., Tao, Y., Shao, J., Zhang, C., Liu, D., Luo, J., Wang, D., and Yang, Q. H. (2014). "Oriented and interlinked porous carbon nanosheets with an extraordinary capacitive performance," *Chemistry of Materials* 26(23), 6896-6903. DOI: 10.1021/ cm503845q

Article submitted: February 13, 2017; Peer review completed: April 13, 2017; Revised version received and accepted: June 22, 2107; Published: July 5, 2017.
DOI: 10.15376/biores.12.3.5928-5941